High-Performance Organic Field-Effect Transistors Based on π-Extended Tetrathiafulvalene Derivatives

ARTICLE *in* JOURNAL OF THE AMERICAN CHEMICAL SOCIETY · AUGUST 2005

Impact Factor: 12.11 · DOI: 10.1021/ja051755e · Source: PubMed

J|A|C|S
COMMUNICATIONS

Published on Web 06/29/2005

High-Performance Organic Field-Effect Transistors Based on π-Extended Tetrathiafulvalene Derivatives

Naraso,[†] Jun-ichi Nishida,[†] Shinji Ando,[†] Jun Yamaguchi,[‡] Kenji Itaka,[‡] Hideomi Koinuma,[‡] Hirokazu Tada,[§] Shizuo Tokito,[⊥] and Yoshiro Yamashita*,[†]

Department of Electronic Chemistry, Interdisciplinary Graduate School of Science and Engineering, Tokyo Institute of Technology, Nagatsuta, Midori-ku, Yokohama 226-8502, Materials and Structures Laboratory, Tokyo Institute of Technology, Nagatsuta, Midori-ku, Yokohama 226-8503, Institute for Molecular Science, Myodaiji, Okazaki 444-8787, NHK Science and Technical Research Laboratories, Kinuta, Setagaya-ku, Tokyo 157-851, Japan

Received March 19, 2005; E-mail: yoshiro@echem.titech.ac.jp

Organic field-effect transistors (OFET) have recently attracted considerable attention for electronic applications such as low-cost integrated circuits and flexible displays.[1] Charge carrier mobility, on/off ratio, threshold voltage, and stability are important key factors that determine the FET performances.[2] Over the recent 20 years, thiophene oligomers[3] and acene molecules[4] have been extensively studied. Recently, tetrathiafulvalene (TTF) derivatives were reported to exhibit excellent FET performances in single crystals.[5] However, because of the strong electron-donating properties of TTFs, their thin films are labile to oxygen, resulting in poor FET performances in thin films.[6] To enhance the air stability, decrease of the electron-donating property is necessary. This is considered to be achieved by introducing fused benzene rings to the TTF skeleton. Electron-deficient nitrogen heterocycles such as pyrazine are expected to further reduce the electron-donating property. Another advantage of using such fused aromatic rings is to increase intermolecular π−π interactions, leading to a large transfer integral between molecules, which is crucial for high carrier mobility.[7] Therefore, we have now fabricated the FET devices of dibenzoTTF **1**, dinaphthoTTF **2**, dipyrazinoTTF **3**, and diquinoxalinoTTF **4** and have investigated the relationship between the FET characteristics and structures.

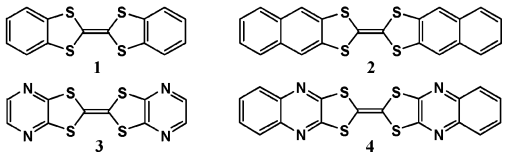

The TTF derivatives **1**−**4** were prepared according to the reported methods.[8] The oxidation potentials were measured by cyclic voltammetry.[9] The first oxidation potentials are as follows: TTF (0.35 V), **1** (0.60 V), **2** (0.72 V), **3** (1.02 V), **4** (1.15 V). Introduction of fused benzene rings increases the oxidation potentials, and that of fused pyrazine rings further increases them. Increase of oxidation potentials means the decrease of the electron-donating properties, which would enhance the stability to oxygen. The HOMO−LUMO energy gaps obtained from the end absorptions (in chlorobenzene) are 2.40, 2.47, 2.44, and 2.11 eV for **1**, **2**, **3**, and **4**, respectively. Among these TTF derivatives, only **2** exhibited photoluminescence at 413 nm in DMF and at 510 nm in the solid state. The large difference indicates the presence of strong intermolecular interactions in the solid state of **2**.

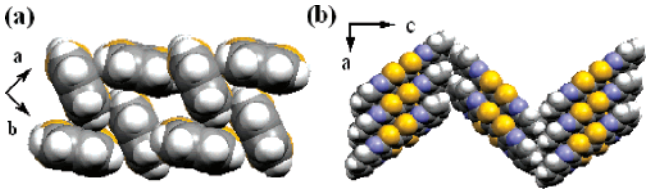

Figure 1. (a) Cystal structure of **2**. (b) Cystal structure of **4**. (Yellow, blue, gray, and white are sulfur, nitrogen, carbon, and hydrogen atoms, respectively).

Table 1. FET Characteristics of **1**−**4** Films

cmpd	device geometry	T_{sub}, °C	mobility, $cm^2 V^{-1} s^{-1}$	on/off ratio	V_{th}/V
1	bottom contact	25	0.06	10^4	26
2	bottom contact	25	0.38	1.6×10^2	10
	bottom contact	80	0.22	3.0×10^2	10
	top contact[a]	25	0.42	6.0×10^3	13
3	bottom contact	25	3.3×10^{-5}	10^5	35
	bottom contact	50	no gate effect		
4	bottom contact	25	1.0×10^{-4}	10^6	38
	bottom contact	80	0.08	10^4	25
	top contact[b]	80	0.2	10^6	36

[a] With OTS treated SiO_2. [b] With Al_2O_3 substrate.

The molecular and crystal structures were determined by single-crystal X-ray structure analysis. The herringbone-type crystal structure of compound **1** has already been reported.[5b] Single crystals of **2**, **3**, **4** suitable for structural analysis were obtained by slow sublimation. The dinaphtho derivative **2** has herringbone packing as shown in Figure 1a. An intermolecular short S···S contact of 3.62 Å is observed between the neighboring TTF molecules, and the shortest intermolecular C−H distance is 2.87 Å. The dipyrazino derivative **3** is also packed in a herringbone manner (see Supporting Information). On the other hand, the quinoxalino derivative **4** has a face-to-face π-stacking motif as shown in Figure 1b, where the interplanar distance is about 3.41 Å and the shortest intermolecular S···S distance is 3.58 Å. The 1,3-dithiole rings are overlapped with the pyrazine rings, suggesting the presence of intermolecular charge-transfer interaction which might induce the face-to-face π stacking.

The FET devices were fabricated with bottom or top contact geometry. All the devices showed p-type behavior. The FET characteristics are summarized in Table 1. The FET performances of tricyclic systems **2** and **4** are higher than those of bicyclic systems **1** and **3**. This is attributed to the more extended π conjugation in the formers. In the bottom contact geometry, the derivatives **1** and **2** exhibited high mobilities of 0.06 and 0.38 $cm^2 V^{-1} s^{-1}$ at room temperature, whereas the derivatives **3** and **4** showed lower mobilities. At higher substrate temperatures, only the mobility of **4** was increased (0.08 $cm^2 V^{-1} s^{-1}$ at 80 °C). No FET performance

[†] Department of Electronic Chemistry, Interdisciplinary Graduate School of Science and Engineering, Tokyo Institute of Technology.
[‡] Materials and Structures Laboratory, Tokyo Institute of Technology.
[§] Institute for Molecular Science.
[⊥] NHK Science and Technical Research Laboratories.

10.1021/ja051755e CCC: $30.25

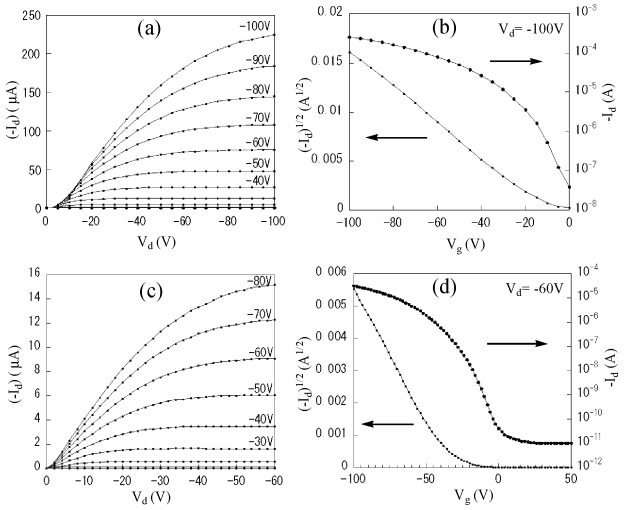

Figure 2. Drain-source current (I_{ds}) versus drain-source voltage (V_{ds}) characteristics: (a) for a FET of **2** on OTS-modified SiO_2 (T_{sub} = 25 °C); (c) for a FET of **4** on Al_2O_3 (T_{sub} = 80 °C). I_d and $I_d^{1/2}$ versus V_g plots: (b) for the **2**-FET and (d) for the **4**-FET. The field-effect mobilities calculated in the saturation regime are 0.42 $cm^2\ V^{-1}\ s^{-1}$ for **2** and 0.2 $cm^2\ V^{-1}\ s^{-1}$ for **4**.

of **3** at 50 °C may be attributed to the disorder orientation because no X-ray diffraction (XRD) pattern was observed. The heterocycle-fused TTFs **3** and **4** have larger on/off ratios than **1** and **2**, suggesting that the stability of films is increased by the electron-accepting units. The higher FET performances of **2** and **4** were obtained from the top contact geometry. For dinaphthoTTF **2**, the FET device was fabricated on SiO_2 substrate. For diquinoxalinoTTF **4**, Al_2O_3 provided higher mobilities than SiO_2.[11] Graphs a and c of Figure 2 show the drain current (I_d) versus voltage (V_d) characteristics for the FET devices of **2** and **4**. The hole mobility of the film **2** calculated in the saturation regime was found to be 0.42 $cm^2\ V^{-1}\ s^{-1}$ (Figure 2 b). As shown in Figure 2d, the mobility of film **4** calculated in the saturation regime was 0.2 $cm^2\ V^{-1}\ s^{-1}$, and the on/off ratio was also a high value of 10^6. The threshold voltages of **4** are higher than those of **2**, which is probably due to the higher oxidation potential of **4**. The thin film of **4** did not degrade in air, and the dependence of the field-effect mobility of **4** under the oxygen pressure was investigated to show the stability. As the oxygen pressure increases from 10^{-7} to 760 Torr, the FET characteristics of the thin films are almost unchanged (see Supporting Information). Under the 760 Torr of O_2 pressure, the mobility was a little increased and the off-current was unchanged. The stability to oxygen can be attributed to the electron-accepting property of quinoxaline.

The films of these TTF derivatives deposited on SiO_2/Si substrates were investigated by XRD in reflection mode (Figure 3). Sharp reflections up to the fourth order are observed, indicating formation of lamellar ordering and crystallinity on the substrate. The d-spacing of **2** obtained from the first reflection peak is 1.76 nm. Since the molecular length of **2** obtained from the single-crystal X-ray analysis is 1.77 nm, this molecule is considered to stand almost perpendicular to the substrate. On the other hand, the thin-film XRD pattern of **4** deposited at room temperature showed a d-spacing of 1.406 nm. Since the molecular length of **4** is 1.739 nm, the molecules are considered to have ca. 36° declining orientation on the substrate. Interestingly, when the substrate temperature is raised to 80 °C, the primary d-spacing increased to 1.744 nm which is similar to the molecular length. This change in the XRD pattern is consistent with the significant change of the mobility upon raising the substrate temperature (from 1×10^{-4} to

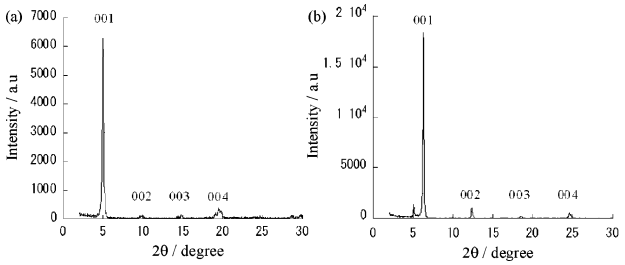

Figure 3. X-ray diffraction of films (50-nm thickness) deposited at room temperature (a) for **2** and (b) for **4**.

0.08 $cm^2\ V^{-1}\ s^{-1}$).[12] AFM images (see Supporting Information) revealed that the thin film of **4** deposited at 80 °C consists of uniformly arranged grains, whereas the thin film deposited at room temperature has a rough surface. This morphological change is also consistent with the marked improvement of the FET characteristics.

In conclusion, introduction of aromatic rings to the TTF skeleton was effective to enhance the intermolecular interactions, leading to excellent p-type FET performances in thin films. A π-stacking structure was constructed by using electron-accepting quinoxaline rings, which was also useful to enhance the stability of the FET device to oxygen. Fabrication of new FETs based on related TTF and tetraselenafulvalene (TSF) derivatives is currently underway.

Acknowledgment. This work was supported by The 21st Century COE program, a Grant-in-Aid for Scientific Research on Priority Areas (No. 15073212), and Nano-technology Support Project from the Ministry of Education, Culture, Sports, Science and Technology, Japan.

Supporting Information Available: The FET device fabrication, molecular packing diagrams of **2**−**4**, O_2 pressure dependence of I_d versus V_d characteristics of **4**, XRD patterns of **1** and **3**, AFM images of **4** (PDF); X-ray crystallographic data in CIF format. This material is available free of charge via the Internet at http://pubs.acs.org.

References

(1) (a) Katz, H. E.; Bao, Z.; Gilat, S. L. *Acc, Chem. Res.* **2001**, *34*, 359−369. (b) Facchetti, A.; Yoon, M.-H.; Stern, C. L.; Katz, H. E. Marks, T. J. *Angew. Chem., Int. Ed.* **2003**, *42*, 3900−3903. (c) Dimitrakopoulos, C. D.; Malenfant, P. R. L. *Adv. Mater*. **2002**, *14*, 99−117.

(2) (a) Moon, H.; Zeis, R.; Borkent, E. J.; Besnard, C.; Lovinger, A. J.; Siegrist, T.; Kloc, C.; Bao, Z. *J. Am. Chem. Soc.* **2004**, *126*, 15322−15323. (b) Xue, J.; Forrest, S. R. *Appl. Phys. Lett.* **2001**. *79*, 3714−3716.

(3) (a) Facchetti, A.; Deng, Y.; Wang, A.; Koide, Y.; Sirringhaus, H.; Marks, T. J.; Friend, R. H. *Angew. Chem., Int. Ed*. **2000**, *39*, 4547−4551. (b) Facchetti, A.; Mushrush, M.; Katz, H. E.; Marks, T. J. *Adv. Mater*. **2003**, *15*, 33−38. (c) Facchetti, A.; Letizia, J.; Yoon, M.-H.; Mushrush, M.; Katz, H. E.; Marks, T. J. *Chem. Mater*. **2004**, *16*, 4715−4727.

(4) (a) Afzali, A.; Dimitrakopoulos, C. D.; Breen, T. L. *J. Am. Chem. Soc.* **2002**, *124*, 8812−8813. (b) Sakamoto, Y.; Suzuki, T.; Kobayashi, M.; Gao, Y.; Fukai, Y.; Inoue, Y.; Sato, F.; Tokito, S. *J. Am. Chem. Soc.* **2004**, *126*, 8138−8140.

(5) (a) Mas-Torrent, M.; Durkut, M.; Hadley, P.; Ribas, X.; Rovira, C. *J. Am. Chem. Soc.* **2004**, *126*, 984−985. (b) Mas-Torrent, M.; Hadley, P.; Bromley, S. T.; Crivillers, N.; Veciana, J.; Rovira, C. *Appl. Phys. Lett.* **2005**, *86*, 012110.

(6) Noda, B.; K, Mao.; Aoyagi, I.; Mori, T.; Taguchi, T.; Kambayashi, T.; Ishikawa, K.; Takezoe, H. *Chem. Lett.* **2005**, *34*, 392−393.

(7) (a) Curtis, M. D.; Cao, J.; Kampf, J. W. *J. Am. Chem. Soc.* **2004**, *126*, 4318−4328. (b) Koren, A. B.; Curtis, M. D.; Francis, A. H.; Kampf, J. W. *J. Am. Chem. Soc*. **2003**, *125*, 5040−5050.

(8) (a) Nakayama, J.; Seki, E.; Hoshino, M. *J. Chem. Soc., Perkin. Trans. I* **1978**, 468−471. (b) Papavassiliou G. C.; Yiannopoulos, S. Y.; Zambounis, J. S. *Chem. Scr*. **1987**, *27*, 265−268.

(9) Cyclic voltammograms were measured in PhCN containing 0.1 mol dm^{-3} $TBAPF_6$. The Pt disk, Pt wire, and SCE were used as the working, counter, and reference electrodes, respectively.

(10) Deposition of **1** on a heated substrate was unsuccessful because this compound sublimed at the high temperature.

(11) The mobility carried out by top-contact configuration of compound **4** deposited on SiO_2 was 6.3×10^{-3} $cm^2\ V^{-1}\ s^{-1}$ (T_{sub} = 80 °C). The lower mobility may be due to the unfavorable orientation of molecules on the substrate.

(12) The driving force for the phase transition of compound **4** at 80 °C is still unclear.

JA051755E